EUCHEMBIOJ

The European Chemistry and Biotechnology Journal
Eur. Chem. Biotechnol. J. **2: 27-38** (2024)

RESEARCH ARTICLE

# A comparative study of glutathione-coated iron oxide and glutathione-coated core-shell magnetic nanoparticles for their antiviral activities

Pinar Sen [1*] | Sevda Demir [1] | Bekir Can Altindisogullari [1] | Fikrettin Sahin [1]

[1] Yeditepe University, Department of Genetics and Bioengineering, Faculty of Engineering, **Istanbul, 34755, Turkey**
* **Corresponding author**: E-mail: sen_pinar@hotmail.com; Ph.: +90 216 578 0619.

**Citation:** Sen, P., Demir, S., Altindisogullari, B.C., & Sahin, F. (2024). Comparative study of glutathione-coated iron oxide and glutathione-coated core-shell magnetic nanoparticles for their antiviral activities. The European chemistry and biotechnology journal, 2, 27-38. https://doi.org/10.62063/ecb-22



**Peer review:** Externally peer reviewed.

**Received:** 11.04.2024
**Accepted:** 28.05.2024
**Published:** 25.07.2024

## Abstract

Iron oxide nanoparticles and its nanocomposites have attracted attention because of their potential applications in biomedicine. Here, firstly the $Fe_3O_4$ nanoparticles were prepared and then Ag was deposited by reducing the Ag salt onto the surface of the $Fe_3O_4$ nanoparticles. This way, bimetallic nanoparticles were obtained. The synthesized nanoparticles were characterized using ultraviolet-visible absorption spectroscopy, transmission electron microscopy and X-ray diffraction and the size and surface charge of the nanoparticles were determined by the dynamic light scattering (DLS) and zeta potential. The spectrographic data demonstrated the size of the glutathione-coated $Fe_3O_4$ nanoparticles to be 4.48 nm and glutathione-coated core-shell magnetic nanoparticles to be 7.98 nm with the spherical morphology and well monodispersed. This study was also designed to investigate the inhibitory effect of Ag@$Fe_3O_4$-GSH, $Fe_3O_4$-GSH and glutathione (GSH) against Human Herpes Simplex Virus Type 1 (HSV-1), Human Adenovirus Type 5, Human Poliovirus Type 1, and Bovine coronavirus. The significant inhibition of Ag@$Fe_3O_4$-GSH was observed against Poliovirus (4 Log), Adenovirus (3 Log), and HSV-1 (2 Log), respectively. GSH showed remarkable antiviral effect against Bovine coronavirus (3 Log) while it exhibited log reduction (1 Log) against HSV-1 and poliovirus. $Fe_3O_4$-GSH showed a reduction of 1 Log only for RNA viruses such as poliovirus and bovine coronavirus. These results demonstrate promising antiviral activity, highlighting the potential of these nanoparticles in combating viral infections.

**Keywords**: Adenovirus, antiviral activity, BCoV, glutathione, HSV-1, iron oxide nanoparticles, magnetic nanoparticles, nanocomposites, poliovirus.

## Introduction

Nanotechnology combines various areas of science. Many nanomaterial types have been introduced up to now, for various applications. Among them, magnetic nanoparticles are of great interest for researchers in biomedical science, catalysis and environmental remediation (Elliott & Zhang, 2001; Govan & Gunko, 2014; Gupta & Gupta, 2005). The iron oxide (II, III) based magnetic nanoparticles are the most promising among the other magnetic nanoparticles (Antone et al., 2019). In particular, $Fe_3O_4$ magnetite nanoparticles have recently attracted great attention due to their different features compared to individual nanoparticles and took place greatly in materials science, biochemistry and diagnostics (Nguyen et al., 2021). Magnetic iron oxide nanoclusters have unique properties, because they combine the properties of individual nanoparticles and exhibit collective behavior through interactions between individual nanoparticles (Kostopoulou & Lappas, 2015). In addition to this, magnetic iron oxide nanoparticles ($Fe_3O_4$ NPs) offer unique properties such as abundance, low toxicity and chemical and photochemical stability, making them an attractive material for usage in certain applications (Naseem & Durrani, 2021). The behaviors of these nanoclusters can be enhanced by the capping molecules leading to novel functional materials. Numerous studies have been conducted on the passivation of iron oxide nanoparticles using capping agents to control the morphology and shape (Mbuyazi & Ajibade, 2023). Besides the synthesis of homogeneous core magnetic $Fe_3O_4$ NPs, advanced nanoarchitectures such as core–shell and composites have been highlighted in biomedical applications (Zhang et al., 2006). For this aim, silver nanoparticles (AgNPs) were used to functionalize the $Fe_3O_4$ NPs as inorganic supports constructing the core-shell structure. Immobilization of Ag NPs on the surface of $Fe_3O_4$ NPs has been shown to limit the aggregation of nanostructure, which renders the applicability of the structures in related applications (Kumari et al., 2019).

Glutathione (GSH) is a water-soluble tripeptide composed of the amino acids and known to function directly or indirectly in many important biological phenomena. GSH plays an important role in plants, mammals, fungi and some prokaryotic organisms as a detoxification agent (Townsend et al., 2003). Several *in vivo* studies have reported the efficiency of this kind of antioxidant substances against viral infections. It was observed that the introduction of GSH reduced some viral infections (Palamara et al., 1996). Although the antiviral activity of antioxidant substances has been demonstrated clearly, the big handicap is that some molecules, such as GSH, are not freely transported into most cells. For this reason, we aimed to combine the target drug with the drug carrier system, allowing easier access to the membranes of many cell types. Magnetic iron oxide and silver nanoparticles as combined or individually have been used in many applications, but GSH coated derivatives of two different nanoparticles will be the first example of *in vivo examination.* Incidences of emerging infections have posed serious public health. Although infectious outbreaks can be controlled within a few years, new dangers of infectious diseases will likely depend on evolving and re-emerging infections. Moreover, viral infections caused by the development of antiviral drug-resistant strains have posed a serious threat globally, resulting in high mortality and economic burden, especially in immunocompromised patients (Parvez & Parveen, 2017). Therefore, it is important to develop new antiviral drugs with a different mode of action than those currently in use.

In our study, glutathione (GSH) functionalized $Fe_3O_4$ NPs ($Fe_3O_4$-GSH) and glutathione functionalized AgNPs immobilized on $Fe_3O_4$ NPs to obtain Ag@$Fe_3O_4$-GSH as core-shell nanoparticles were obtained. Later, the antiviral activities of the two nanostructures and GSH were examined against different DNA (Human Herpes Simplex Type 1 and Human Adenovirus Type 5) and RNA (Human Poliovirus Type 1, and Bovine Coronavirus) viruses.

# Materials and methods

### *Chemicals and instruments*

Iron acetylacetonate, benzyl ether, oleic acid, oleylamine, 1,2-Hexadecanediol, ethanol, acetone, chloroform ($CHCl_3$), methanol, glutathione (GSH), $Ag(ac)_3$, tetramethylammonium hydroxide (TMAOH) were purchased from Sigma–Aldrich. Ultra-pure water was from MilliQ water. Size determination and zeta potential using dynamic light scattering (DLS) was performed using a Nano-ZS instrument (Malvern Instruments Ltd, Malvern, UK). Electronic spectra were recorded on a PerkinElmer LAMBDA 25 Series UV−vis spectrophotometer with a quartz cell of 1 cm. The morphologies of the $Fe_3O_4$-GSH and Ag@$Fe_3O_4$-GSH core shell nanoparticles were assessed using transmission electron microscope (TEM) JEOL JEM-2100Plus 200kV. X-ray diffraction (XRD) data were collected over the 2θ = 10–100◦ range using a Bruker D-8 Advance diffractometer, under Cu Kα radiation (λ = 1.5405 Å, 40kV - 40 mA ).

### *Synthesis*

The $Fe_3O_4$-GSH was synthesized as outlined in the literature with a slight modification, in two steps (Robinson et al., 2010). In the first step, iron acetylacetonate (0.71 g, 2 mmol) was dissolved in benzyl ether (20 mL) with oleic acid (2 mL, 6 mmol) and oleylamine (2 mL, 4 mmol) under $N_2$ with vigorous stirring. 1,2-Hexadecanediol (2.58 g, 10 mmol) was added into the solution and heated under reflux for 2 hours, then cooled to room temperature. The resultant magnetite NPs were separated by precipitation with ethanol (10 mL) and cleaned with acetone. Finally, the product was dried using a vacuum oven at 50 °C. In the second step, $Fe_3O_4$ NPs (0.5 g) suspension in a mixed liquid of $CHCl_3$ (15 mL) and methanol (5 mL) was sonicated for 20 minutes. Then, glutathione (0.4 g) dissolved in water (5 mL) was added to the solution, and sonication method was applied to the final colloidal solution for 2 hours. Then, the mixture was precipitated with ethanol and washed few times with ethanol and water, dried in oven at 50 °C, yielding the final magnetic $Fe_3O_4$-GSH NPs.

The Ag@$Fe_3O_4$-GSH was synthesized as reported in the literature with slight modification in three steps (Bankole & Nyokong, 2016; Robinson et al., 2010). After applying the same first step for the preparation of $Fe_3O_4$ -GSH, the prepared bare $Fe_3O_4$ NPs (0.5 g), Ag(ac)3 (0.83 g, 2.2 mmol), 1,2-hexadecanediol (3.1 g, 12 mmol), oleic acid (0.5 mL, 1.5 mmol) and oleylamine (3 mL, 6 mmol) were added to benzyl ether (30 mL) under N2 flow with vigorous stirring. The reaction solution was heated to 180–190 °C and held at this temperature for 1.5 hours. After cooling to room temperature, ethanol was added into the solution and the magnetic material collected by precipitation. The precipitated product was washed with ethanol and re-dispersed in 15 mL of TMAOH solution. Glutathione (0.125 g) in 2 mL degassed water was added to the NP solution and sonicated for 40 minutes to allow for ligand exchange to take place. Water soluble glutathione functionalized Ag@$Fe_3O_4$ NPs (Ag@$Fe_3O_4$-GSH) were precipitated and washed with ethanol and water to remove unbounded GSH from the surface of the NPs. Finally, the obtained nanoparticles were dried under vacuum at 50 °C.

### *Cell culture and viruses*

Green monkey kidney cells (Vero-CCL81, ATCC) were used for analyses of human herpes simplex type 1 (MacIntyre, Zeptometrix), Adenovirus type 5 (Adenoid 75-, ATCC), *Poliovirus type 1, (LSc 2ab, ATCC).* Madin Darby Bovine Kidney Cells (MDBK-NBL-1, ATCC) were used for *Bovine coronavirus*

*(Mebus, ATCC)* analysis. All cell lines and viruses were obtained from the Genetic and Bioengineering Department of Yeditepe University, (Istanbul, Turkey).

***Cytotoxicity assay and antiviral activity***

Cytotoxicity assay and antiviral activity studies were based on Spearman-Kärber method (Ramakrishnan, 2016) and EN14476 European standard method. Briefly, for cytotoxicity assay, Vero cells were seeded $4x10^4$ cell/well in 96 well plate with DMEM-H and incubated at 37 ºC, 5% $CO_2$ incubator for 24 hours. Then, cells were treated with *Log10* serial dilution of Ag@$Fe_3O_4$-GSH, $Fe_3O_4$-GSH and GSH and incubated at 37 ºC 5% $CO_2$ incubator for 24 hours to determine maximum nontoxic dose (MNTD). Vero cells were seeded based on the same procedure for monolayer formation in each well to determine antiviral activity. Viruses were diluted based on *Log10* serial dilution with virus medium (1% PSA, MEM, Gibco) and the material MNTD applied on them for 15 minutes. Then, old media was removed from cell monolayer and washed with PBS three times. The mixture of the virus and nanoparticles and GSH were transferred on to cells and incubated for 72 hours. At the end of the incubation period, the cytopathic effect (CPE) due to the viral infection was evaluated under an inverted microscope. Results were calculated with the following formulas; where X k refers to highest dilution dose, d: represents the difference between dilutions, n represents the number of wells per dilution, r: (-) is the sum of the answers, Mv is the value of antiviral activity, Lg (Vc) refers to the logarithmic average of virus control biological replicates and Lg (Va) is the logarithmic average of experimental biological replicates.

$$M= Xk + d \times [0.5 – (1/n) \times (r)] \quad [1]$$

$$Mv = Lg(Vc) - Lg(Va) \quad [2]$$

# Results and discussion

The $Fe_3O_4$-GSH NPs were synthesized in benzyl ether as organic solvent with oleic acid and oleylamine, resulting in surface coated with hydrophobic ligands. This was followed by the ligand exchange procedure to obtain the coated with GSH (Robinson et al., 2010). The Ag@$Fe_3O_4$-GSH NPs were obtained with a two step procedure, including the formation of the $Fe_3O_4$ NPs first, followed by the reduction of a silver salt in order to add a layer of Ag on the iron oxide NPs, which was dissolved in benzyl ether. This core-shell nanoparticles were then functionalized with GSH (Bankole & Nyokong, 2016; Robinson et al., 2010). Ultraviolet-visible (UV-vis) absorption spectroscopy and X-ray diffraction (XRD) were used to detect the presence of Ag in the NPs and transmission electron microscopy (TEM) was employed to determine the morphology of the $Fe_3O_4$-GSH NPs and Ag coated $Fe_3O_4$ NPs. Dynamic light scattering (DLS) was utilized to demonstrate the size of each nanoparticle and zeta potential measurement was used to see the charge of the each nanoparticle.

***TEM micrographs***

The transmission electron microscope (TEM) was applied to determine the morphologies and shape of the $Fe_3O_4$-GSH and Ag@$Fe_3O_4$-GSH, as shown in Figure 1. The TEM micrograph for $Fe_3O_4$-GSH showed almost mono dispersed, non-aggregated, quasi-spherical shape particles. Upon capping of $Fe_3O_4$ with silver to form Ag@$Fe_3O_4$-GSH NPs, in addition to small, transparent and evenly dispersed $Fe_3O_4$ grains, some large, dark-colored Ag NP grains were obtained, and further aggregation was observed as compared to the pure $Fe_3O_4$-GSH NPs.

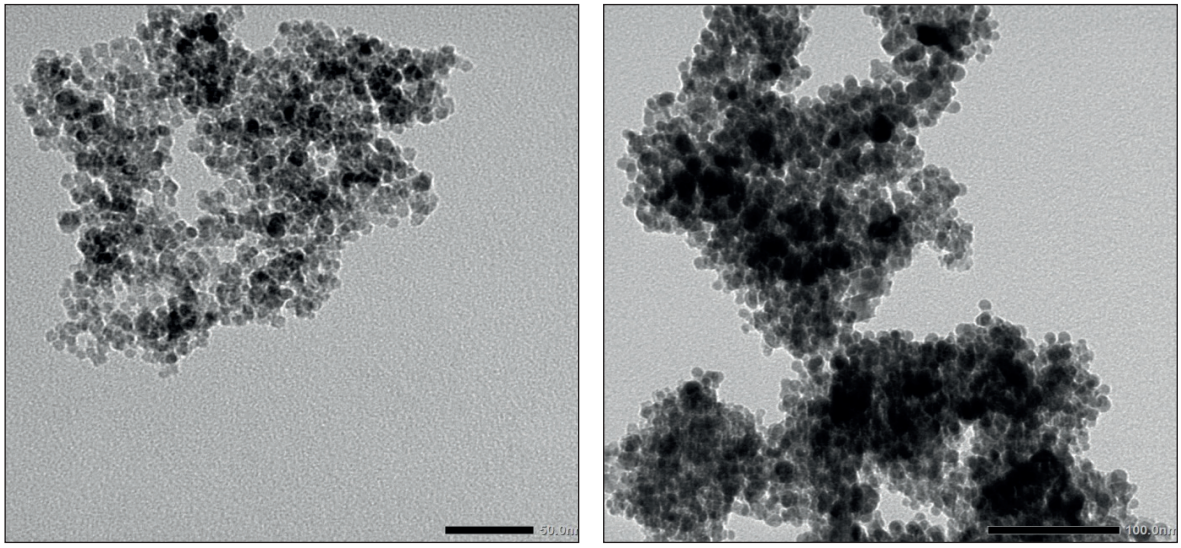

(a) (b)

**Figure 1.** TEM images of a) $Fe_3O_4$-GSH, b) Ag@$Fe_3O_4$-GSH.

***Dynamic light scattering (DLS) spectra and zeta potential***

DLS was used for the determination of particle size for both type of the nanoparticles (Figure 2). The average size determined by DLS was 4.48 nm for $Fe_3O_4$-GSH. The size increased to 7.98 nm for Ag@$Fe_3O_4$-GSH, which indicated the successful surface coating of silver for $Fe_3O_4$ nanoparticles.

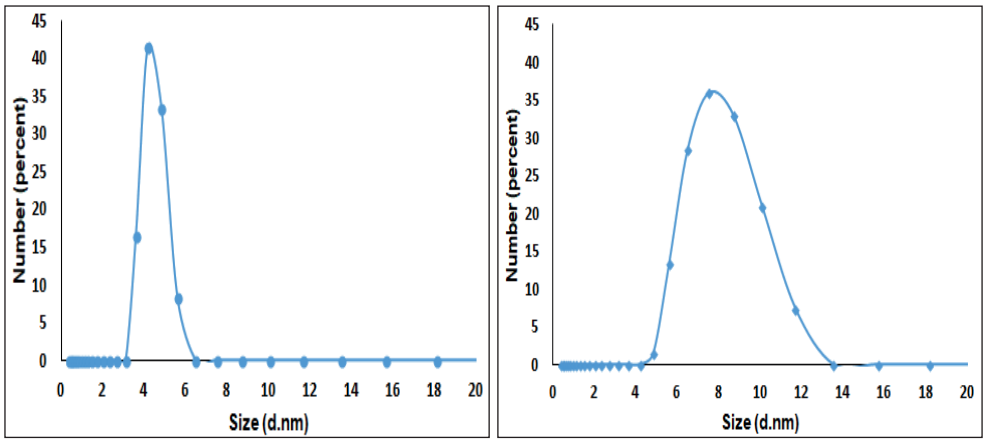


(a) (b)

**Figure 2.** DLS graph showing average particle size of a) $Fe_3O_4$-GSH, b) Ag@$Fe_3O_4$-GSH.

Zeta potential measurements allow us to evaluate the colloidal stability in solution, as well as NPs surface charge. Surface charges of the studied nanoparticles are shown in the zeta potential graphs (Figure 3). The zeta potential value was determined as -19 mV for $Fe_3O_4$-GSH and -35.7 mV for Ag@ $Fe_3O_4$-GSH in ethanol suspension. The huge negative surface charge of the Ag@$Fe_3O_4$-GSH shows its higher stability due to the repulsive force among particles (Khashan et al., 2017).

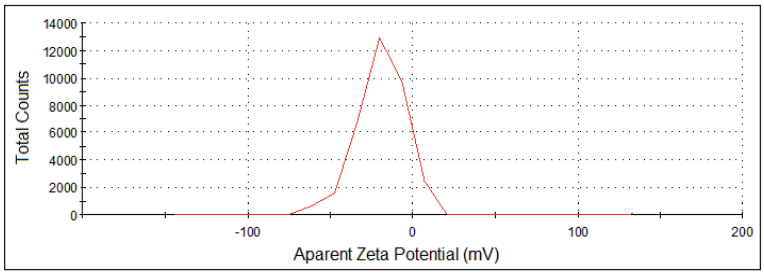


(a)

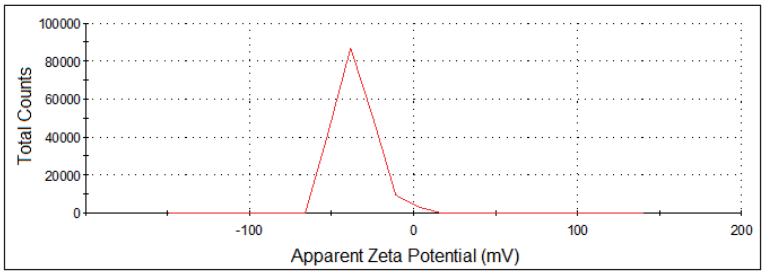


(b)

**Figure 3.** Zeta potential of a) $Fe_3O_4$-GSH, b) Ag@$Fe_3O_4$-GSH dispersed in ethanol.

### *X-ray diffraction (XRD)*

XRD was employed for investigation of crystallinity of the prepared NPs and XRD patterns of $Fe_3O_4$-GSH nanoparticles and Ag@$Fe_3O_4$-GSH core-shell nanoparticles, as shown in Figure 4. The observed characteristic diffraction peaks for $Fe_3O_4$ ($2\theta$= 30.2, 35.5, 43.0, 54.2, 56.7 and 62.4°) can be assigned to diffraction of $Fe_3O_4$ crystal with an inverse spinal structure (Malekia et al., 2020). The XRD diffraction patterns of the Ag@$Fe_3O_4$-GSH nanoparticles showed well-defined crystalline peaks at $2\theta$= 30.3, 35.7, 38.3, 44.3, 53.8, 57.1, 63.01, 64.5, 77.5 and 81.6°. The peaks that are characteristic of silver at 38.3, 44.3, 64.5, 77.5 and 81.6° corresponding to the face centered-cubic structure of metallic silver were not observed for $Fe_3O_4$-GSH NPs due to the presence of the Ag shell on the magnetic NPs and the other peaks at $2\theta$=30.3, 35.7, 53.8, 57.1 and 63.01° were similar crystalline peaks, which are shifted compared to the $Fe_3O_4$-GSH NPs crystalline planes.

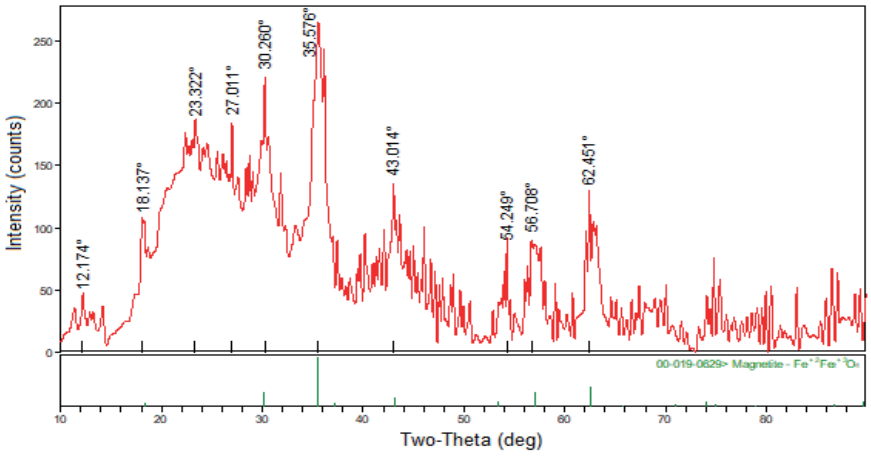


(a)

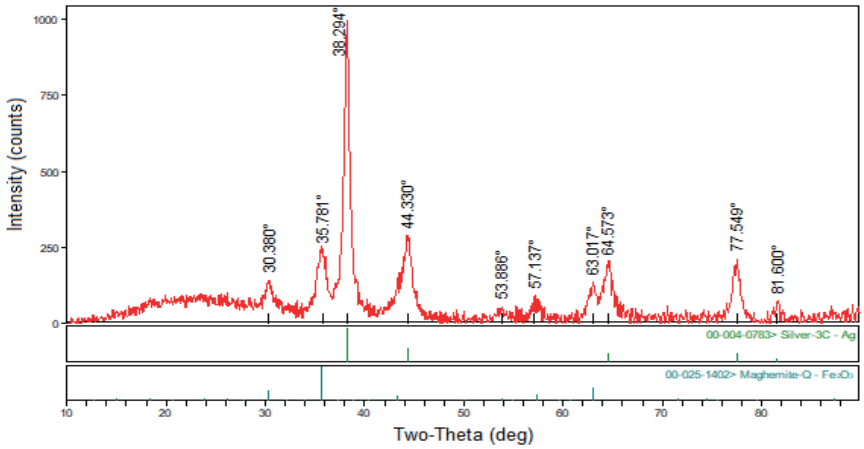


(b)

**Figure 4.** X-ray diffraction patterns of a) $Fe_3O_4$-GSH, b) Ag@$Fe_3O_4$-GSH.

### *Optical properties*

The UV–vis absorption spectrum was applied to characterize the synthesized nanoparticles (Figure 5). The optical absorption spectra of the $Fe_3O_4$-GSH exhibit absorption peak at around 250 nm. This peak is related to the electrons moving from the oxygen atom to the d-metal orbital (Ramesh et al., 2017). The large bump in absorption spectrum of Ag@$Fe_3O_4$-GSH NPs at around 480 nm was due to resonant excitation of surface plasmons (SPR) of the Ag surface (Xu et al., 2006).

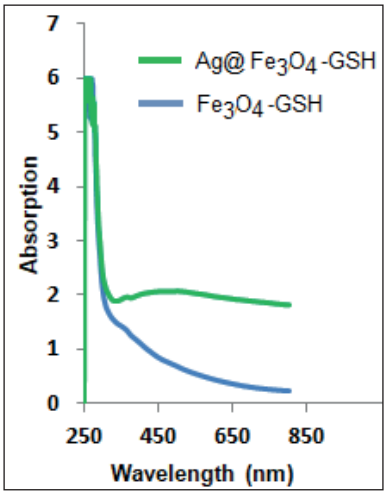


**Figure 5.** UV–Visible absorption spectrum of $Fe_3O_4$-GSH NPs and Ag@$Fe_3O_4$-GSH NPs.

***Antiviral activity***

Antiviral activity analysis can be performed for screening and evaluating viral entry inhibition, viral genome replication blocking and viral maturation inhibition (Rumlová & Ruml, 2017). In this research, antiviral activities of Ag@$Fe_3O_4$-GSH, $Fe_3O_4$-GSH and GSH were evaluated for viral entry inhibition. Ultimately, significant inhibition was observed with Ag@$Fe_3O_4$-GSH against Poliovirus (4 Log), Adenovirus (3 Log), and HSV-1 (2 Log). GSH exhibited remarkable antiviral effects against Bovine coronavirus (3 Log) and showed a log reduction of 1 Log against HSV-1 and Poliovirus. $Fe_3O_4$-GSH demonstrated a reduction of 1 Log, particularly against RNA viruses, such as Poliovirus and Bovine coronavirus (Table 1). Among these, only Ag@$Fe_3O_4$-GSH nanoparticles have an antiviral effect against all type of viruses at least 99%, while their activity against Bovine coronaviruses was 90%. This situation demonstrates that GSH and $Fe_3O_4$ molecules, when combined with silver to form Ag@$Fe_3O_4$-GSH nanoparticles, exhibit a synergistic effect against human DNA and RNA viruses. However, synergistic effect was not observed against bovine coronavirus. This can be attributed to host differences, variations in viral membrane proteins, and diversity in host receptors (Teissier et al., 2011). Studies have shown that a deficiency in glutathione, a potent antioxidant, can lead to the accumulation of reactive oxygen species (ROS) in cells, potentially resulting in immune suppression and faster progression of infections (Khanfari & Al Qaroot, 2020). The obtained results regarding glutathione support this information. This is because glutathione alone demonstrates a reduction of 1 log against HSV-1 and Poliovirus, and a reduction of 3 logs against bovine coronavirus, particularly enhancing its efficacy against human viruses in nanoparticle form. Given that bovine coronavirus belongs to the same family as SARS-CoV-2 and is considered as a model virus for SARS-CoV-2 in the literature (Naqvi et al., 2020), it is believed that glutathione, either alone or in combination with human host cells, may also exhibit antiviral activity against SARS-CoV-2.

Although it has been revealed that GSH depletion plays a role in a wide variety of viral infections (Beck et al., 2000) and nanoparticles made of silver can be effective antiviral agents against varieties such as HIV-1 (Sun et al., 2005), hepatitis B virus (Lu et al., 2008), herpes simplex virus type 1 (Baram-Pinto et al., 2009), influenza virus (Papp et al., 2010), the antiviral activity of GSH coated silver nanoparticles as shell around the magnetic nanoparticle core have not been reported.

| **Table 1.** *In vitro* antiviral activity of the studied samples.

| *Compounds* | Log reduction | | | |
|---|---|---|---|---|
| | HSV-1 | Adenovirus | Poliovirus | BCoV |
| **Ag@$Fe_3O_4$-GSH** | 2 | 3 | 4 | 1 |
| **$Fe_3O_4$-GSH** | - | - | 1 | 1 |
| **GSH** | 1 | - | 1 | 3 |

## Conclusions

The antiviral activity of iron oxide nanoparticles against HSV-1, poliovirus, adenovirus and bovine coronavirus were investigated. In order to see the capping agent (GSH) effect over the studied viruses, GSH was also investigated. Among the prepared magnetic nanoparticles, the nanoparticles containing a magnetic core and a silver shell (Ag@$Fe_3O_4$-GSH) exhibited remarkable activity than the bare magnetic nanoparticles ($Fe_3O_4$-GSH).

## Acknowledgements

We are thankful to the Department of Genetic and Bioengineering, Yeditepe University for providing necessary facilities to carry out the experiment of this work.

## Conflict of interest

The authors declare no conflict of interest.

## Data availability statement

Data can be obtained from the corresponding author upon a reasonable request.

## Ethics committee approval

Ethics committee approval is not required for this study.

## Authors' contribution statement

**Study conception and design**: P.S.; **Data collection**: P.S. S.D., B.C.A., **Analysis and interpretation of results**: P.S., S.D., B.C.A., F.S.; **Manuscript draft preparation**: P.S., S.D., B.C.A., F.S. All authors reviewed the results and approved the final version of the manuscript.

**ORCIDs and emails of the authors**

Pinar Sen | ORCID 0000-0002-3181-9890 | sen_pinar@hotmail.com

Sevda Demir | ORCID 0000-0003-0427-3519 | sevda.demir@yeditepe.edu.tr

Bekir Can Altindisogullari | ORCID 0000-0002-2753-6046 | bekir.can@yeditepe.edu.tr

Fikrettin Sahin | ORCID 0000-0003-3993-1630 | fsahin@yeditepe.edu.tr

## References


Antone, A.J., Sun, Z., & Bao, Y. (2019). Preparation and Application of Iron Oxide Nanoclusters. *Magnetochemistry*, 5, 45. https://doi.org/10.3390/magnetochemistry5030045

Bankole, O.M., & Nyokong, T. (2016). Comparative studies on photophysical and optical limiting characterizations of low symmetry phthalocyanine linked to $Fe_3O_4$–Ag core–shell or hybrid nanoparticles. *New journal of chemistry,* 40, 10016-10027. https://doi.org/10.1039/c6nj01511e

Baram-Pinto, D., Shukla, S., Perkas, N., Gedanken, A., & Sarid, R. (2009). Inhibition of herpes simplex virus type 1 infection by silver nanoparticles capped with mercaptoethane sulfonate. *Bioconjugate chemistry,* 20, 1497–1502. https://doi.org/10.1021/bc900215b

Beck, M.A., Handy, J., & Levander, O.A. (2000). The role of oxidative stress in viral infections. *Annals of the new york academy of sciences*, 917, 906–912. https://doi.org/10.1111/j.1749-6632.2000.tb05456.x

Govan, J., & Gunko Y.K. (2014). Recent Advances in the Application of Magnetic Nanoparticles as a Support for Homogeneous Catalysts. *Nanomaterials,* 4, 222-241. https://doi.org/10.3390/nano4020222

Gupta, A.K., & Gupta, M. (2005). Synthesis and surface engineering of iron oxide nanoparticles for biomedical applications. *Biomaterials,* 26, 3995–4021. https://doi.org/10.1016/j.biomaterials.2004.10.012

Elliott, D.W., & Zhang, A. (2001). Field Assessment of NanoscaleBimetallic Particles for Groundwater Treatment. *Environmental science and technology,* 35, 4922-4926. https://doi.org/10.1021/es0108584

Khashan, S., Dagher, S., Tit, N., Alazzam, A., & Obaidat, I. (2017). Novel Method for Synthesis of $Fe_3O_4$@$TiO_2$ Core/Shell Nanoparticles. *Surface and coating technology,* 322, 92-98. https://doi.org/10.1016/j.surfcoat.2017.05.045

Khanfari, A., & Al Qaroot, B. (2020). Could glutathione depletion be the Trojan horse of COVID-19 mortality?. *European Review for Medical and Pharmacological Sciences,* 24, 12500-12509.

Kostopoulou, A., & Lappas, A. (2015). Colloidal magnetic nanocrystal clusters: Variable length-scale interaction mechanisms, synergetic functionalities and technological advantages. *Nanotechnology reviews*, 2015, 4, 595–624. https://doi.org/10.1515/ntrev-2014-0034

Kumari, M., Gupta, R., & Jain, Y. (2019). $Fe_3O_4$–Glutathione stabilized Ag nanoparticles: A new magnetically separable robust and facile catalyst for aqueous phase reduction of nitroarenes. *Applied organometallic chemistry,* 33, 5223. https://doi.org/10.1002/aoc.5223

Lu, L., Sun, R.W. Chen, R., Hui, C.K., Ho, C.M., Luk, J.M., Lau, G.K., & Che, C.M. (2008). Silver nanoparticles inhibit hepatitis B virus replication. *Antiviral therapy,* 13, 253–262. https://doi.org/10.1177/135965350801300210

Malekia, B., Esmaeilnezhad, E., Choi, H.J., Koushkid, E., Aliabad, H.A.R., & Esmaeili, M. (2020). Glutathione-capped core-shell structured magnetite nanoparticles: Fabrication and their nonlinear optical characteristics. *Current applied physics*, 20, 822–827. https://doi.org/10.1016/j.cap.2020.03.020

Mbuyazi, T.B., & Ajibade, P.A. (2023). Influence of Different Capping Agents on the Structural, Optical, and Photocatalytic Degradation Efficiency of Magnetite ($Fe_3O_4$) Nanoparticles. *Nanomaterials,* 13, 2067. https://doi.org/10.3390/nano13142067

Nguyen, M.D., Tran, H., Xu, S., & Lee, T.R. (2021). $Fe_3O_4$ Nanoparticles: Structures, Synthesis, Magnetic Properties, Surface Functionalization, and Emerging Applications. *Applied sciences,* 11, 11301. https://doi.org/10.3390/app112311301

Naqvi, A.A.T., Fatima, K., Mohammad, T., Fatima, U., Singh, I.K., Singh, A., Atif, S.M., Hariprasad, G., Hasan, G.M., & Hassan, I. (2020). Insights into SARS-CoV-2 genome, structure, evolution, pathogenesis and therapies: Structural genomics approach. *BBA - Molecular basis of disease,* 1866, 1658. https://doi.org/10.1016/j.bbadis.2020.165878

Naseem, T., & Durrani, T. (2021). The role of some important metal oxide nanoparticles for wastewater and antibacterial applications: A review. *Environmental chemistry and ecotoxicology,* 3, 59–75. https://doi.org/10.1016/j.enceco.2020.12.001

Palamara, AT., Perno, C.F, Aquaro, S., Bue, M.C., Dini, L., & Garaci, E. (1996) Glutathione inhibits HIV replication by acting at late stages of the virus life cycle. *AIDS research & human retroviruses,* 12, 1537–1541. https://doi.org/10.1089/aid.1996.12.1537

Papp, I., Sieben, C., Ludwig, K., Roskamp, M., Böttcher, C., Schlecht, S., Herrmann, A., & Haag, R. (2010). Inhibition of influenza virus infection by multivalent sialic-acid-functionalized gold nanoparticles. *Small,* 6, 2900–2906. https://doi.org/10.1002/smll.201001349

Parvez, M.K., & Parveen, S. (2017). Evolution and Emergence of Pathogenic Viruses: Past, Present, and Future. *Intervirology,* 60, 1–7. https://doi.org/10.1159/000478729

Ramakrishnan, M.A. (2016). Determination of 50% endpoint titer using a simple formula. *World Journal of virology,* 5(2), 85-86. https://doi.org/10.5501/wjv.v5.i2.85

Ramesh, R., Geerthana, M., Prabhu, S., & Sohila, S. (2017). Synthesis and Characterization of the Superparamagnetic $Fe_3O_4$/Ag Nanocomposites. *Journal of cluster science,* 28, 963–969. https://doi.org/10.1007/s10876-016-1093-9

Robinson, L, Tung, L.D., Maenosono, S., Walti, C., & Thanh, N.T.K. (2010). Synthesis of core-shell gold coated magnetic nanoparticles and their interaction with thiolated DNA. *Nanoscale,* 2, 2624–2630. https://doi.org/10.1039/c0nr00621a

Rumlová, M., & Ruml, T. (2017). In vitro methods for testing antiviral drugs. *Biotechnology advances,* 36(3), 557–576. https://doi.org/10.1016/j.biotechadv.2017.12.016

Sun, R.W., Chen, R., Chung, N.P., Ho, C.M., Lin, C.L., & Che, C.M. (2005). Silver nanoparticles

fabricated in Hepes buffer exhibit cytoprotective activities toward HIV-1 infected cells. *Chemical communications,* 40, 5059–5061. https://doi.org/10.1039/B510984A

Teissier, E., Penin, F., & Pécheur, E. (2011). Targeting Cell Entry of Enveloped Viruses as an Antiviral Strategy. *Molecules,* 16, 221-250. https://doi.org/10.3390/molecules16010221

Townsend, D.M., Tew, K.D., & Tapiero, H. (2003). The importance of glutathione in human disease. *Biomedicine & pharmacotherapy,* 57, 145–155. https://doi.org/10.1016/S0753-3322(03)00043-X

Xu, G., Chen, Y., Tazawa, M., & Jin, P. (2006). Surface Plasmon Resonance of Silver Nanoparticles on Vanadium Dioxide. *The journal of physical chemistry b*, 110, 2051-2056. https://doi.org/10.1021/jp055744j

Zhang, L., Dou, Y., & Gu, H. (2006). Synthesis of Ag–$Fe_3O_4$ heterodimeric nanoparticles. *Journal of colloid and interface science*, 297, 660–664. https://doi.org/10.1016/j.jcis.2005.11.009